INL/RPT-22-69979
Revision 0

Status of Research Activities on LVDTs: Modeling and Simulation Development and Performance Characterization of Commercial LVDTs

October 2022

Milestone M2CT-22IN0702064

Kurt Davis, Austin Fleming, and Malwina Wilding
Idaho National Laboratory

Zhangxian Deng, Alex Draper, and Joshua Poorbaugh
Boise State University

Idaho National Laboratory

INL is a U.S. Department of Energy National Laboratory
operated by Battelle Energy Alliance, LLC

INL/RPT-22-69979
Revision 0

Status of Research Activities on LVDTs: Modeling and Simulation Development and Performance Characterization of Commercial LVDTs

Milestone M2CT-22IN0702064

Kurt Davis, Austin Fleming, and Malwina Wilding
Idaho National Laboratory
Zhangxian Deng, Alex Draper, and Joshua Poorbaugh
Boise State University

November 2022

Idaho National Laboratory
Idaho Falls, Idaho 83415

http://www.inl.gov

Prepared for the
U.S. Department of Energy
Office of Nuclear Energy
Under DOE Idaho Operations Office
Contract DE-AC07-05ID14517

Page intentionally left blank

SUMMARY

FY-22 research focused on two major areas. The first area was modeling and simulation with linked testing that will advance the Linear Variable Differential Transformers (LVDT) technology for use by stakeholders requiring LVDTs in upcoming irradiation tests. The second area focused on testing LVDTs purchased from U.S. suppliers that were investigated in FY-21. These cross-cutting development activities will ensure stakeholders have the current state-of-the-art LVDT-based technologies for deployment in future irradiation tests.

Two stand-alone reports are included in the appendixes. The purpose of this report is to provide a convenient body of work to access the reports and to evaluate the data and conclusions provided.

Appendix A, "Testing of the RDP Translation Transducer," contains a complete evaluation of an RDP Electrosense linear transducer that has the capability of replicating the form, fit, and function of LVDTs currently being used at Idaho National Laboratory (INL).

Appendix B is an extract from the report, "Advanced Sensors and Instrumentation Program at Boise State University (BSU), August 2022, Linear Variable Differential Transformers." This report contains modeling and testing results conducted at BSU and INL.

CONTENTS

FIGURES

Page intentionally left blank

ACRONYMS

BSU	Boise State University
CANDU	Canada Deuterium Uranium
DOE	U.S. Department of Energy
IFE	Institute for Energy
INL	Idaho National Laboratory
LVDT	linear variable differential transformer
PI	principal investigator
RDP	reliability dependability and price
UG	undergraduate

Appendix A

Testing of the RDP Translation Transducer

Appendix A

Testing of the RDP Translation Transducer

A-1. INTRODUCTION

Real-time pressure and dimensional measurements in fuel and fuel cladding during irradiations can be used to understand phenomena such as fuel and cladding elongation, the buildup of "crud," pressurization from fission gas release, and pellet-clad mechanical interactions. These phenomena can adversely affect fuel performance. Therefore, in situ measurements are critical to advancing the knowledge base related to irradiation effects on fuels and cladding. Measurements of these phenomena require micron-scale accuracy to assess fuel performance. Linear Variable Differential Transformers (LVDTs) are well-established sensors that provide such resolution and are known for their superior in-pile performance under irradiation.

The Institute for Energy Technology (IFE) is one of the pioneers in LVDT development for in-pile testing. Since the IFE began taking in-core measurements, over 2,200 different LVDTs have been installed in test rigs in their Halden Boiling Water Reactor. Failure rates of less than 10% after 5 years of operation is expected for their LVDTs operating in boiling water reactor, pressurized-water reactor, or CANDU (Canada Deuterium Uranium) reactor conditions [1,2]. In June of 2018, the Halden Boiling Water Reactor was permanently shut down, and budgets for fuels research and sensor development were eliminated. This action forced IFE to limit the availability of LVDTs. Idaho National Laboratory (INL) and the international in-pile testing community relied heavily on IFE for their supply of LVDTs and corresponding sensors. To mitigate this situation, INL researchers conducted a study [3] to identify potential suppliers of LVDTs that can meet the in-pile testing needs. Two potential suppliers, RDP Electrosense and Newtek Sensor Solutions, were identified, and their sensors were procured for evaluation. This report will document the testing of an RDP Electrosense translation transducer. The testing of the Newtek Sensor Solution LVDT will be documented in a subsequent report. The RDP Electrosense sensor is similar to an LVDT in application, but it has functional differences that need exploring. The following section describes these differences.

A-2. LVDT VS RDP TRANSLATION TRANSDUCER

LVDTs are reliable sensors that convert the mechanical movement of a specimen into an electrical output. A simple schematic of a five-wire LVDT (INL's baseline for in-pile testing) is shown in Figure A-1. Three coils are used, a single primary coil and two secondary coils. An alternating (excitation) current is driven through the primary coil, causing a voltage to be induced in each secondary coil, which is proportional to its mutual inductance with the primary coil. As the core moves, these mutual inductances change, causing voltages induced in the secondary coils to experience a corresponding change. This change is measured using a demodulation function, D, represented by

$$D = (Va - Vb)/(Va+Vb) \quad \text{(A1)}$$

Demodulation can then be correlated to a movement or a change in pressure when the core is attached through a pushrod to a specimen or bellows

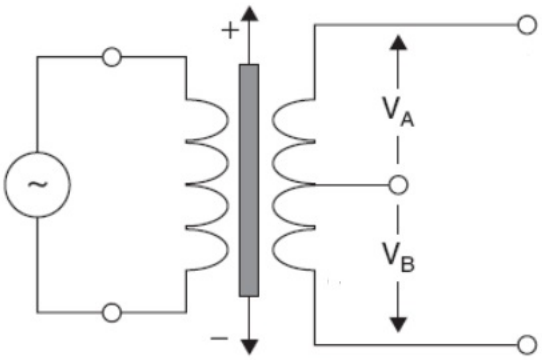

Figure A-1. Five-wire LVDT schematic.

RDP Electrosense produces an off-the-shelf translation transducer. Their transducers are similar in form, fit, and design to an LVDT. Figure A-2 illustrates a simple schematic of the translation transducer they provide. The main difference of their transducer is that it has no primary coil and that the driving signal is injected across what is equivalent to the secondary coils of an LVDT. This transducer uses a half-bridge signal conditioner that produces a ratio function, f(V) = Va/Vb, for the correlation to core movement.

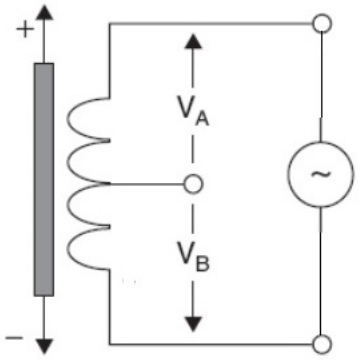

Figure A-2. Schematic for the translation transducer.

A-3. SENSOR TESTING

Testing was conducted using an RDP Electrosense, LIN56 displacement transducer (See Figure A-3). This transducer is 15-mm in diameter and 105-mm in length. This size is slightly larger than typical IFE LVDTs with diameters ranging from 12 mm down to 8 mm. This sensor is rated to 600°C with a translation range of ± 5 mm. It is designed to withstand a radiation dose of 100 G Rad (not irradiated in this test) and pressures to 200 bar at 250°C. This transducer was driven and read by the MOD 600 system also provided by RDP Electrosense (see Figure A-4). The transducer was mounted in the INL calibration rig [4] and tested in the vertical orientation (see Figure A-5). Testing was conducted at atmospheric pressure in ultrapure argon flowing at 2 l/m at temperatures of 20, 300, and 600°C.

Figure A-3. RDP Electrosense, LIN56 transducer body.

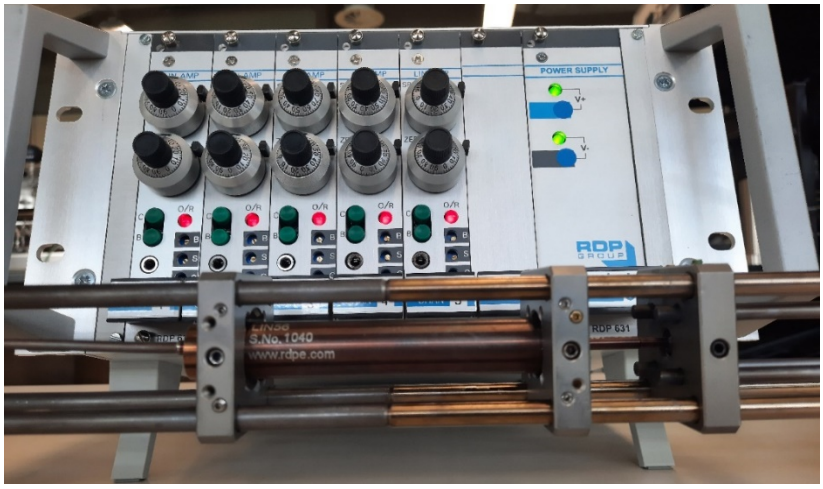

Figure A-4. Testing of the RDP sensor at INL. Shown in photo, MOD 600 System with LIN56 transducer mounted in INL calibration rig's rails.

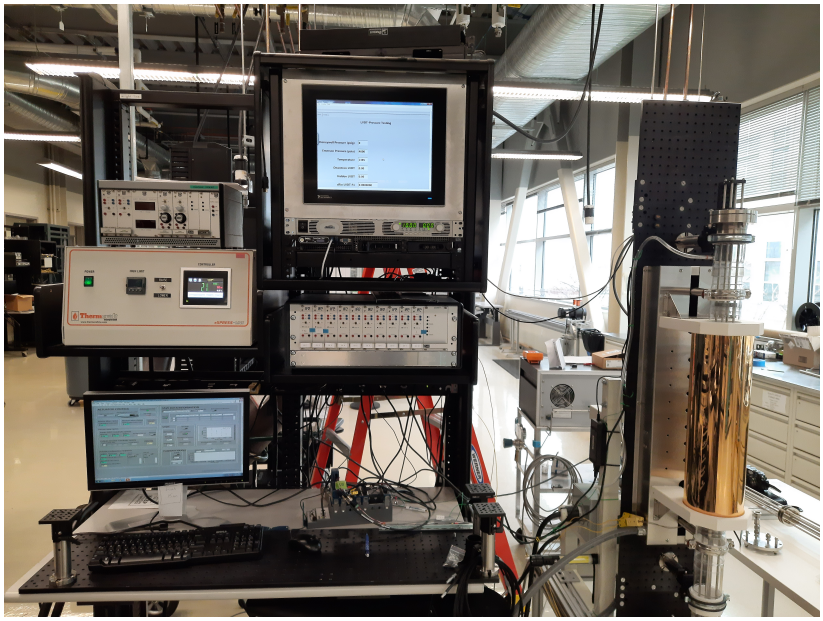

Figure A-5. Testing of the transducer in the INL calibration rig.

Figure A-6 shows the calibration curve developed at 20°C. The full range nonlinearity (percent error at travel extremes) for this calibration was found to be 0.7 which is good compared to the advertised full range nonlinearity of 1.0. Testing was also conducted to determine repeatability and resolution at this temperature. Repeatability was tested by moving the sensor core from the −3 mm position to the 3 mm position. This process was repeated 20 times. The standard deviation for each position was found to be 1.0 µm for the −3 mm position and 1.1 µm for the 3 mm position. Resolution was evaluated by starting at the −3 mm position and then moving three 10 µm steps forward and then three 10 µm steps backward. The nonlinearity was then calculated at each step. Nonlinearity remained uniform over the full range of steps with an average of −1.1 and outliers at −0.8 and −1.2. This method was chosen because of a software limit of 10 µm steps. The uniform nonlinearity suggest that submicron is achievable with this sensor.

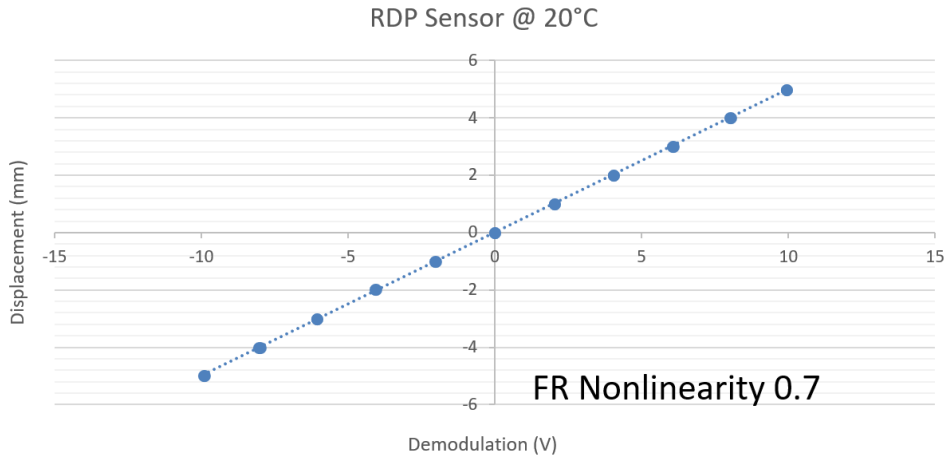

Figure A-6. Calibration data taken at 20°C.

Figure A-7 shows the calibration curve developed at 300°C. The full range nonlinearity for this calibration was found to be 0.9, which is within RDP's advertised full range nonlinearity of 1.0. Testing was also conducted to determine repeatability and resolution at this temperature. Again, repeatability was tested by moving the sensor core from the −3 mm position to the 3 mm position. This process was repeated 20 times. The standard deviation for each position was found to be 7.1 µm for the −3 mm position and 2.1 µm for the 3 mm position. Resolution was evaluated by starting at the −3 mm position and then moving three 10 µm steps forward and then three 10 µm steps backward. The nonlinearity was then calculated at each step. Nonlinearity remained uniform over the full range of steps with an average of 0.5 and outliers at −0.4 and −0.6. The uniform nonlinearity suggest that submicron resolution is achievable with this sensor at 300°C.

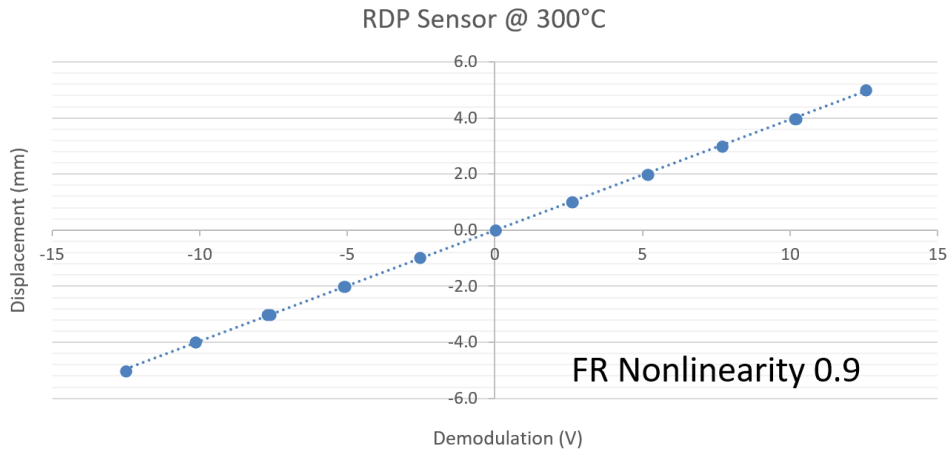

Figure A-7. Calibration data taken at 300°C.

Figure A-8 shows the calibration curve developed at 600°C. The full range nonlinearity for this calibration was found to be 5.8 which is excessive when compared to the RDP's advertised full range nonlinearity of 1.0. The sensor experienced drifting during the 600°C testing. Because of this, repeatability and resolution testing were not conducted. Figure A-9 shows the displacement drift with the sensor locked in a static passion. The sensor experienced a drift exceeding 70 µm during a 46-hour test. Based on this data, it can be interpreted that the sensor would have continued to drift for an extended period. It is possible that at 600°C the LIN56 sensor suffered insulation deterioration resulting in poor performance. There are many things that could have caused this, including manufacturing defects on the coils, poor insulation packing in the body, or weld failures in the body.

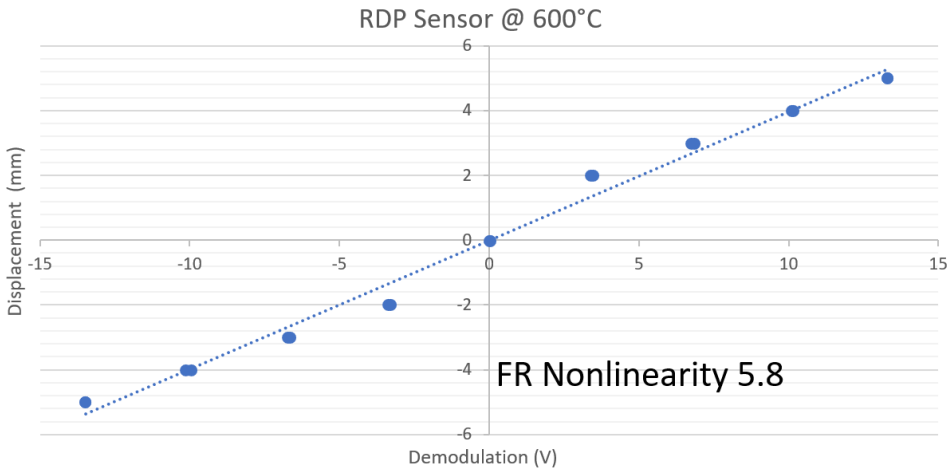

Figure A-8. Calibration data taken at 600°C.

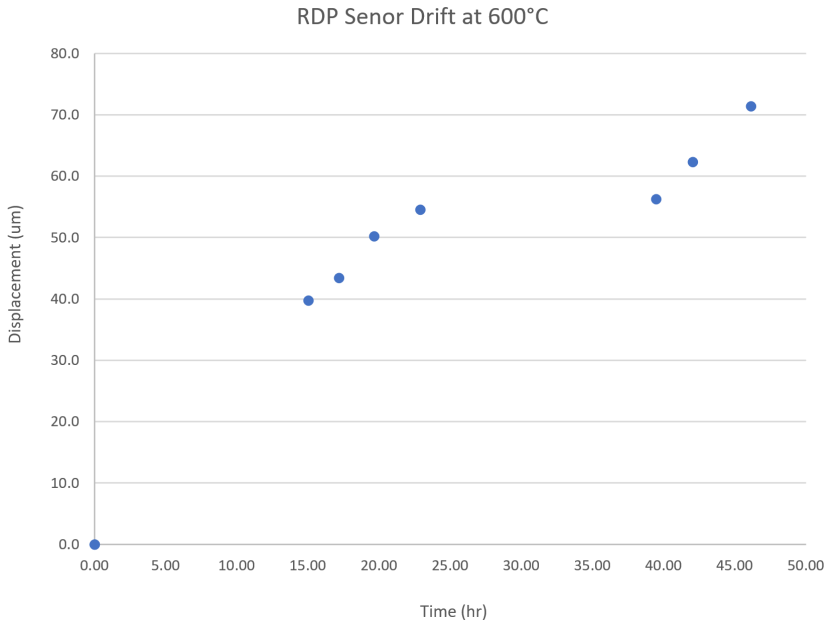

Figure A-9. Drift data taken with the core secured at 600°C.

A-4. CONCLUSIONS

Testing of the LIN56 transducer found that it performed as expected in the 20 to 300°C temperature range. Full range nonlinearity was 0.7 and 0.9 respectively which exceeds the manufacturer's published values. Repeatability and resolution were also found to be acceptable with the 20°C data showing repeatability within 1.1 µm and resolution in the submicron range. The 300°C data showed repeatability within 7.8 µm and submicron resolution was demonstrated.

Testing at 600°C proved to be limiting for this sensor. The full range nonlinearity of 5.8 exceeded the published data of 1.0. Sensor drift prevented full testing.

Further testing is warranted. Manufacturers data suggest that this sensor should have operated to 600°C. Investigation into the cause of the sensor failure is needed. Other LIN56 sensors should be tested to find the limiting temperature for this sensor.

A-5. REFERENCES

1. Solstad, S., and R. V. Nieuwenhove, "Instrument Capabilities and Developments at the Halden Reactor Project," Proceedings of the ANS NPIC HMIT 2009 Topical Meeting on Nuclear Plant Instrumentation, Controls, and Human Machine Interface Technology, Knoxville, TN. (2009).
2. K. L. Davis, D. L. Knudson, J. L. Rempe, J. C. Crepeau and S. Solstad, "Design and Laboratory Evaluation of Future Elongation and Diameter Measurements at the Advanced Test Reactor," Nuclear Technology, 191: 92–105 (2015).
3. K. L. Davis, "Assessment of Supply Chain for Nuclear LVDTs and Related Components Manufacturing," INL-LTD-21-62217, Idaho National Laboratory (2021).
4. C. Jensen, K. Davis, A. Fleming, A. Lambson, K. McCary, K. Tsai, M. Wilding, "FY19 Report for Instrumentation Development for the Transient Testing Program," INL/EXT-19-56000, Idaho National Laboratory (2019).

Appendix B

Advanced Sensors and Instrumentation Program at Boise State University

Appendix B

Advanced Sensors and Instrumentation Program at Boise State University

B-1. LINEAR VARIABLE DIFFERENTIAL TRANSFORMERS

Zhangxian Deng (PI), Alex Draper (UG), Josh Poorbaugh (UG)

B-1.1 Introduction

The mission of the Boise State research team is to use finite element modeling and experimental testing to investigate the thermal drift observed in high-temperature Linear Variable Differential Transformers (LVDT) experiments. It is hypothesized that the thermal drift arises from the thermal strain of LVDT structural materials. To validate this initial hypothesis, this study uses a multiphysics finite element model developed in fiscal year 2021 (FY-21) to design a high-temperature (beyond 300°C) test rig for LVDT at the Measurement Sciences Laboratory. The same test rig will be applicable for future testing in the Transient Reactor Test Facility (TREAT) reactor at Idaho National Laboratory (INL). This report will discuss the design, fabrication, assembly, and preliminary testing of the test rig.

B-1.1.1 Test Rig Design in SolidWorks

The objective is to design a test rig that could accurately control the relative deformation between the soft magnetic core and the coils in an LVDT due to thermal expansion. Figure B-1 shows the conceptual design of the first test rig, in which the magnetic core is locked down by a pair of identical reference materials. In this case, any drift observed in the LVDT would be a result of thermal expansion in LVDT coils or the temperature-driven material property variations of LVDT components. The entire testing body and fixtures were made of 316 stainless steel. Choosing the same material ensures that the testing body expands uniformly at elevated temperatures. 316 stainless steel exhibits superior corrosion resistance and has no impact on the magnetic field distribution as it is non-ferromagnetic.

Figure B-2 shows the final design that was machined and assembled in this study. Because the magnetic core (likely to be silicon steel) expands slower than 316 stainless-steel, the core assembly consisting of two reference material rods and the soft magnetic core undergoes tension. Since both reference rods are made of the same materials and have the same dimensions (both diameter and length), the soft magnetic core is held in position. The LVDT casing is fixed using a set screw in the middle. The coils freely expand to both sides. Therefore, the relative deformation between the soft magnetic core and the LVDT coils should be negligible. By removing the reference material rod on the left (see Figure B-2) and replacing the other reference rod with different materials (e.g., nickel, Inconel), the same test rig would be able to induce different thermal expansions on the magnetic core.

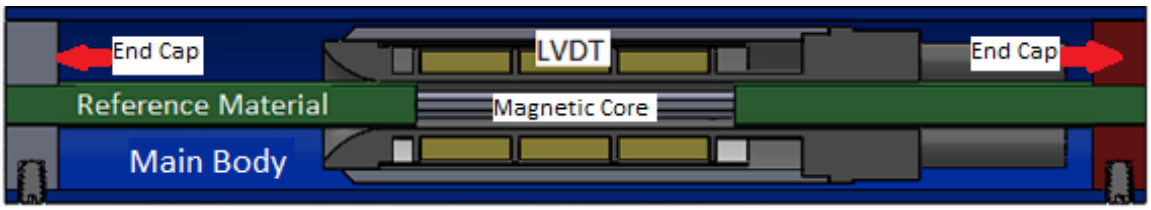

Figure B-1. Original design for the LVDT testing assembly. Body is blue, reference materials are green, end caps are red and grey. LVDT is in the middle with coils shaded yellow.

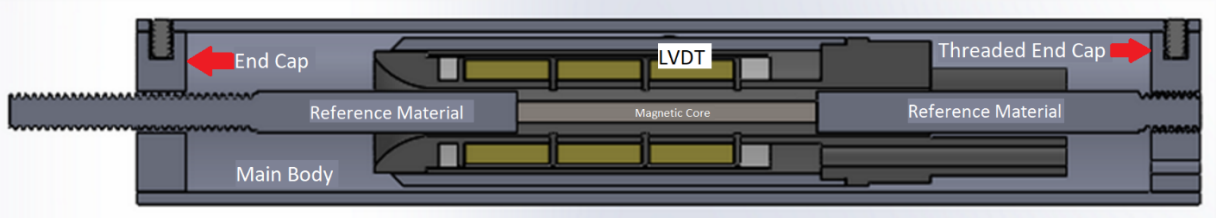

Figure B-2. Cross-section view of updated design with threaded reference materials. On the end that sticks out, a bolt was placed to secure the core in place.

B-1.1.2 Test Rig Simulation in COMSOL

Finite element models for the proposed test rig were created in COMSOL of the proposed test rig at elevated temperatures. These models will validate if the test rig is able to survive the large thermal stress in high-temperature testing.

A two-dimensional (2D) axisymmetric model, as shown in Figure B-3, was developed in FY-21. This model confirmed that the testing body and end caps could survive the large thermal stress beyond 300. However, it does not properly represent the set screw in the actual test rig, because the force provided by the set screw is assumed to be a circumferential surface traction instead of a point load.

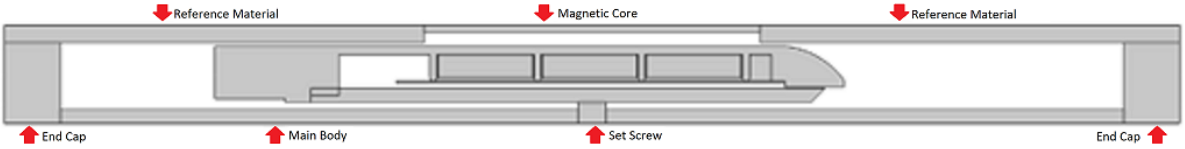

Figure B-3. 2D model of the proposed test rig.

By leveraging the Solidworks LiveLink provided by COMSOL, the actual test rig assembly was also simulated in three-dimensional (3D), as shown in Figure B-4. All threads in the model were simplified into rigidly connected surfaces. To further reduce model complexity, a 120-degree slice was selected that preserved the set screw placements. This model confirmed that the set screw is mechanically strong enough to hold the thermal stress.

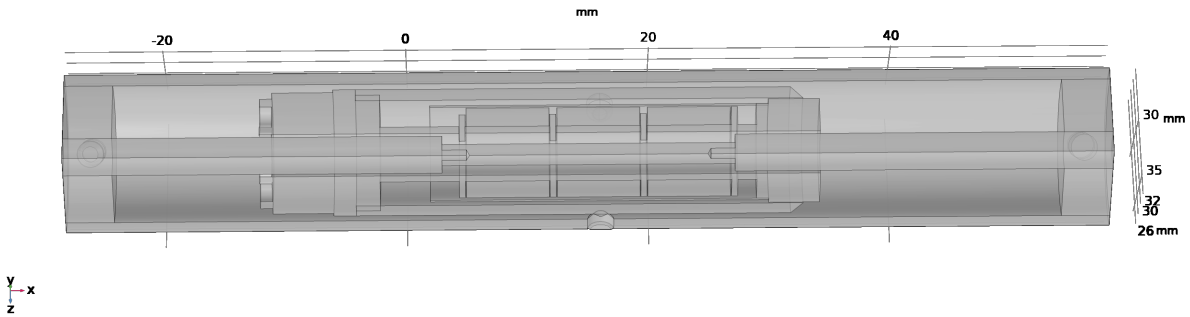

Figure B-4. 3D model of the proposed test rig.

B-1.1.3 Test Rig Machining and Assembly

The outer body has an outer diameter of 15 mm, an inner diameter of 13 mm, and a length of 86 mm. These dimensions were chosen so that the testing assembly would fit in both the testing furnace and the TREAT reactor. All holes on the side of the main body are threaded for 2–56 set screws.

Each end cap has an outer diameter of 13 mm to fit snugly inside the main body, with unthreaded holes in their sides for the set screws to fit into. The threaded end cap has three 1.5-mm holes to facilitate

LVDT wiring and is threaded for a 5–40 type thread. Figure B-5 shows both the machined body and endcaps.

Figure B-5. Main body and machined end caps. The End cap on the left is unthreaded, and the end cap on the right has center thread for the center assembly and wire holes for the LVDT sensor.

Both reference materials were constructed out of 316 stainless steel so that they expand at the same rate as the main body of the testing assembly and can be seen below in Figure B-6. Both reference materials have 5–40 threads on one end, and a 2-mm-long nub 1-mm in diameter to mate them with the magnetic core. The longer reference material is 43-mm long, and the shorter reference material is 33-mm long. Laser welding was conducted at INL to attach all three parts together (as seen in Figure B-6). The right end of the welded rod was threaded into the end cap and the other end is locked down using a nut (as seen in Figure B-2).

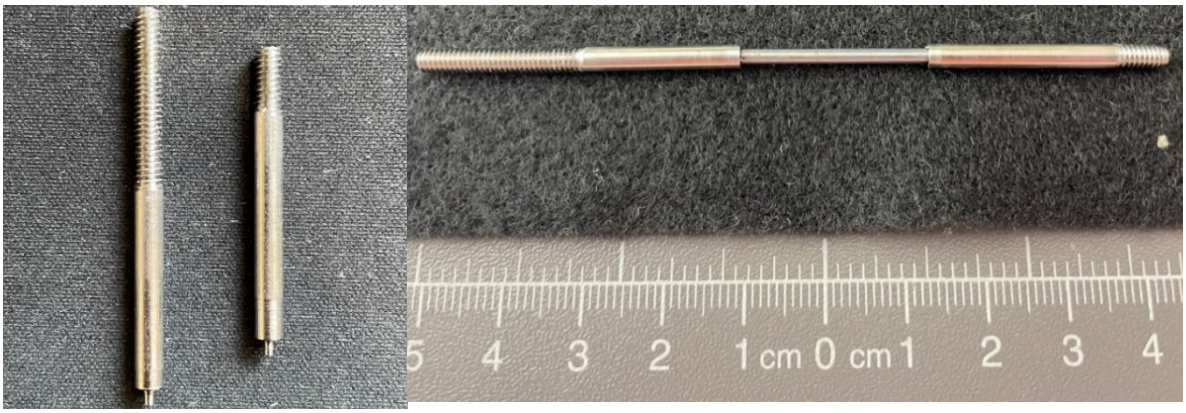

Figure B-6. (Left) Machined reference materials and (right) the final assembly of reference material rods and the magnetic core.

To help with assembly of the test rig, a 3D printed stand (in Figure B-7) and a holding fixture for the LVDT (in brown, below) were fabricated.

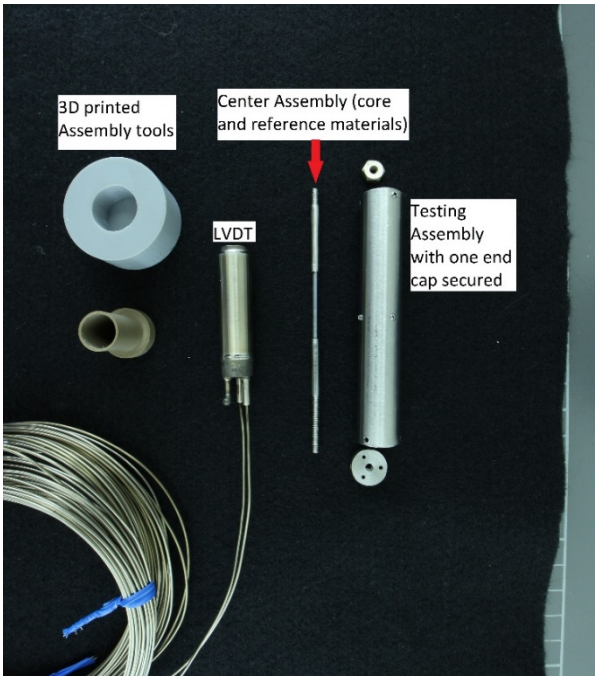

Figure B-7. LVDT test assembly parts before putting them together. 3D printed pieces to help with assembly in upper left.

Following the configuration presented in Figure B-2, the test rig was assembled at INL. Figure B-8 also shows the complete assembly mounted inside the furnace supports before we slid the entire testing apparatus into the furnace. Originally, we planned on securing the testing assembly inside the furnace supports with only one point of contact in the middle. However, when putting it together we mounted it in two spots: at the top and the bottom of the testing assembly. This is a potential source of error as it could interfere with the expansion of the testing assembly.

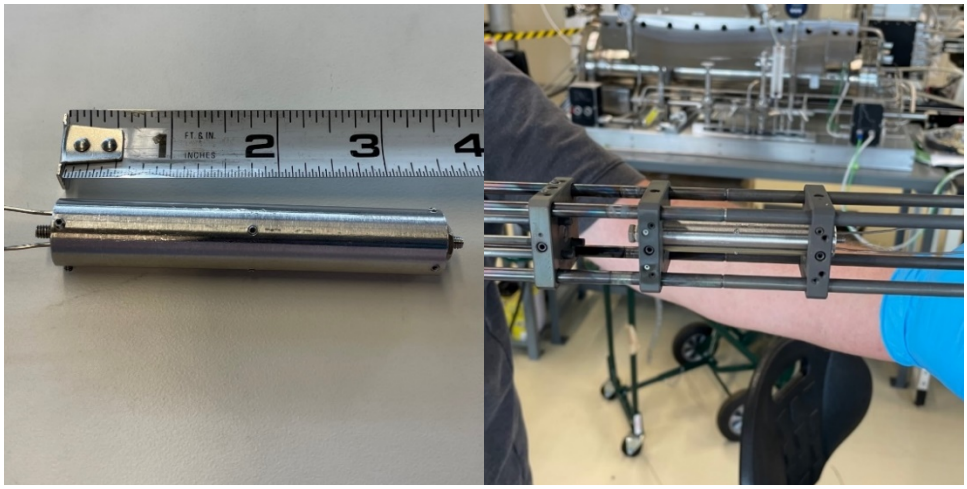

Figure B-8. (Left) Complete test rig ready to be placed in furnace and (right) test rig assembled in furnace supports.

The testing furnace was loaded horizontally before securing the completed assembly in place. Figure B-9 shows how the furnace was tilted vertically and a laminar flow of argon gas was pumped through the furnace before we could begin to heat it up to collect data.

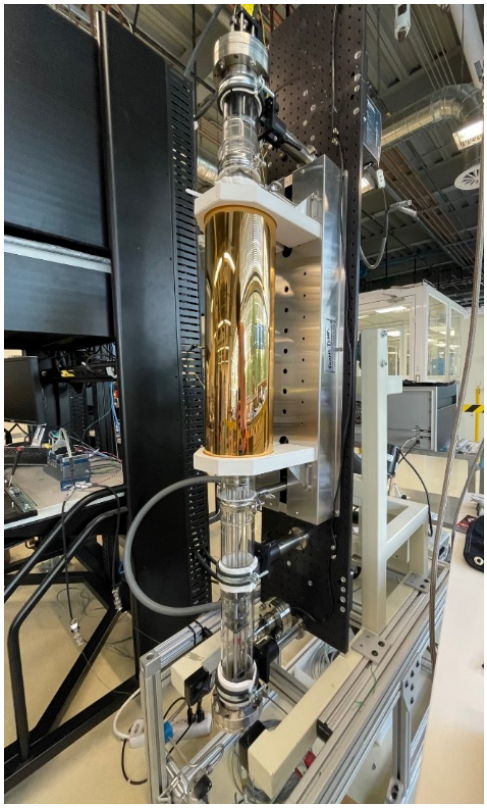

Figure B-9. Vertical furnace with LVDT assembly inside.

B-1.1.4 Data and Results

For runs one and two, the temperature of the furnace and assembly were stepped up from room temperature at 20°C up to 700°C, with different modulated voltage readings taken at different temperatures. Because the temperature of the stainless-steel assembly lags behind the temperature of the furnace, it took 3–4 hours for the system to reach thermal equilibrium where we could start to collect data. For runs one and two, the LVDT assembly was tested while secured in two locations: at the top and the bottom of the testing assembly.

For run three, the furnace was heated up from room temperature at 20°C to 300°C, taking measurements in intervals of 50°C. Additionally, data points were taken without waiting for thermal equilibrium between the testing assembly and the furnace. This procedure could significantly reduce the time consumption without compromising the results. For run three, the mounting of the LVDT test rig on the furnace support was also changed to a single-point fixture (only at the top mount) to allow the free expansion of the LVDT testing body.

Figure B-10 through Figure B-12 show the temperature and modulated voltage for a 10-second interval for runs one two and three respectfully.

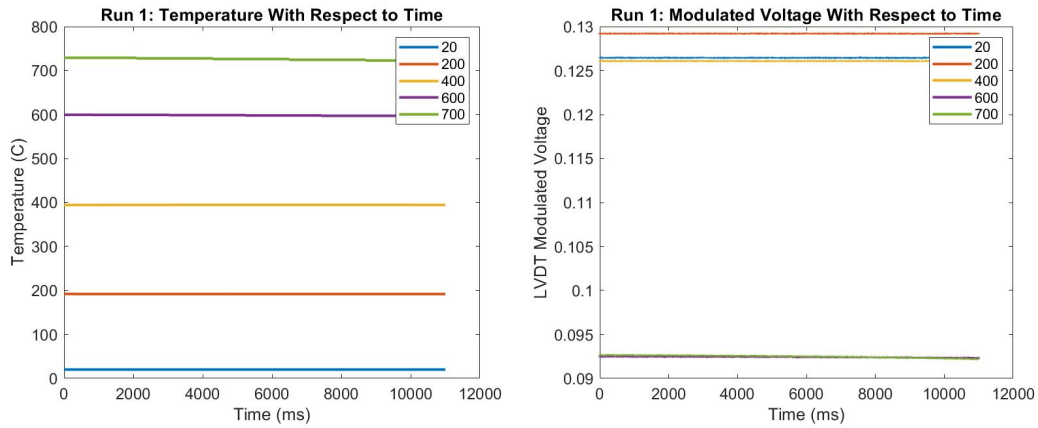

Figure B-10. Temperature and modulated voltage for run one with respect to time.

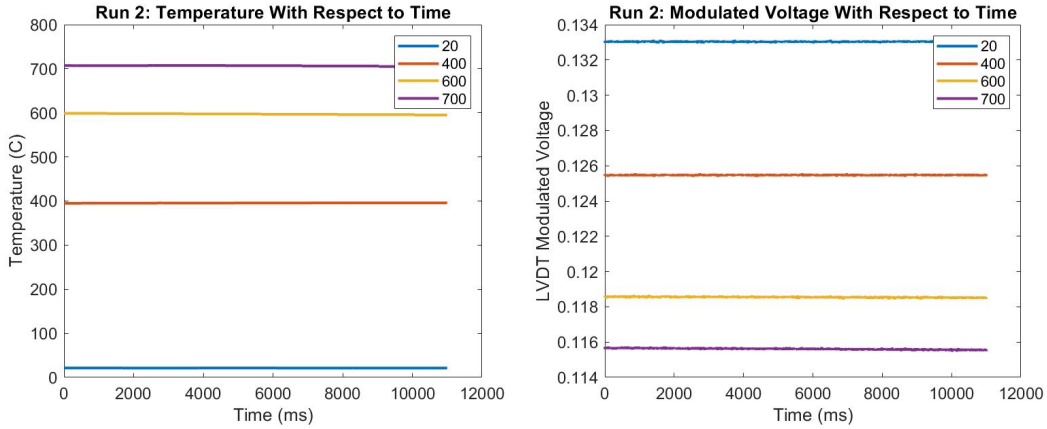

Figure B-11. Temperature and modulated voltage with respect to time for run two.

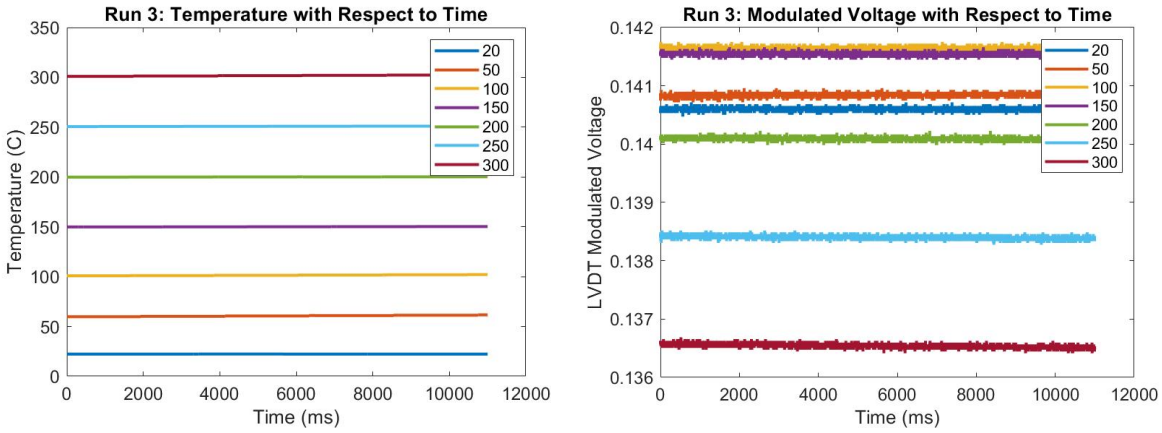

Figure B-12. Temperature and modulated voltage with respect to time for run three.

Figure B-13 shows the modulated voltage with respect to temperature for all runs. Figure B-14 shows the displacement of the core with respect to temperature for all runs. Ideally, if the testing assembly held the core in place and the temperature had no effects on the other LVDT components, the LVDT reading should remain constant regardless of the temperature. If temperature-varying material properties or thermal expansion are the source of LVDT measurement error, then the thermal drift in the LVDT is expected to be linear.

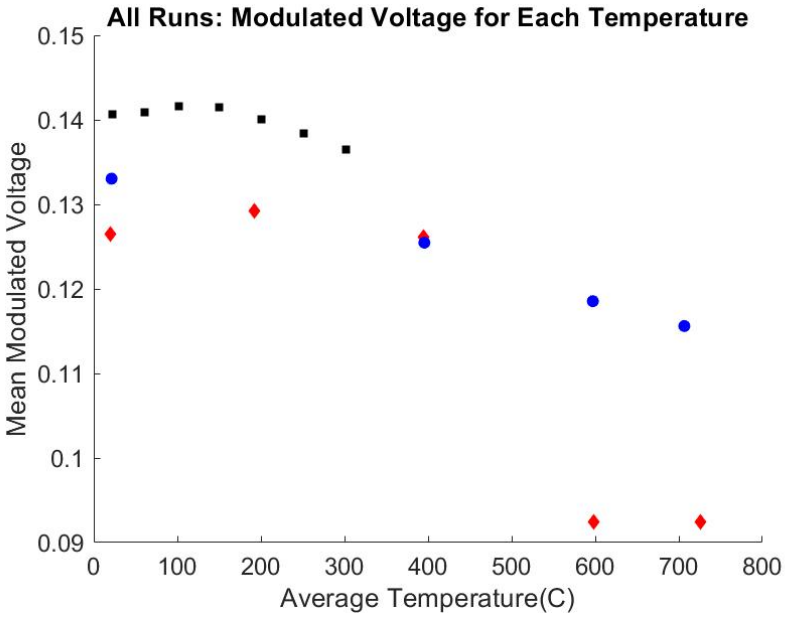

Figure B-13. Mean modulated voltages plotted against temperature for all runs (run one points shown with red diamonds, run two points shown with blue circles, run 3 shown with black squares).

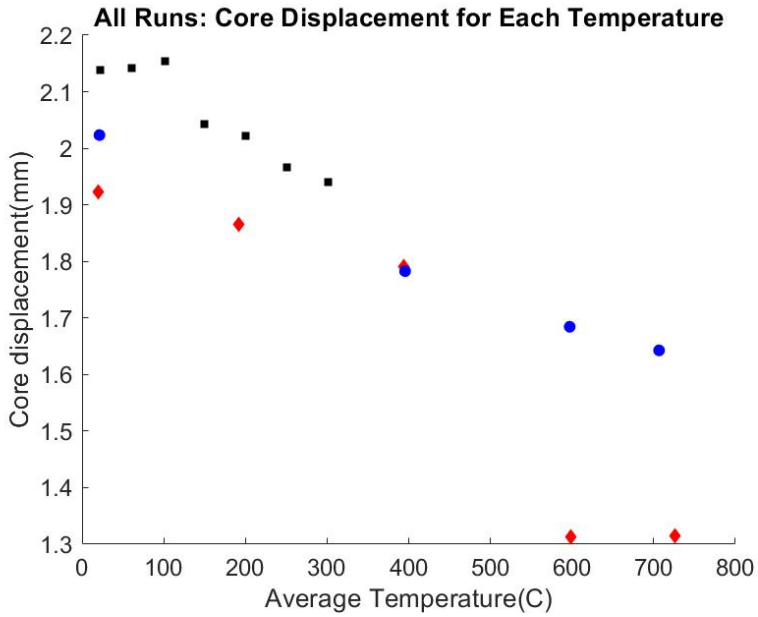

Figure B-14. Core displacement plotted against temperature for all runs (run one points shown with red diamonds, run two points shown with blue circles, run three shown with black squares).

However, from the above figures a significant difference in the values for modulated voltage at each temperature for each of the runs is present, alongside a non-linear spread of the data. This thermal drift is a few orders higher than those observed in previous TREAT reactor tests. While run two showed a somewhat linear decrease in the voltage reading, runs one and three experienced a slight increase in modulated voltage (between 100 to 200°C), before starting to decrease. Another concern is how the starting values for modulated voltage at 20°C varied for each of the three runs. Ideally, the starting position of the core inside the LVDT should remain unchanged, or be the same for each run. We suspect that the welded magnetic core and reference materials were not straight, and the bending of the soft magnetic core at high temperatures was the source of thermal drift. More testing is needed to validate this hypothesis.

B-1.2 Conclusion

This study designed, machined, assembled, and tested a new LVDT test rig to investigate the thermal drift observed in previous TREAT reactor experiments. Based on the hypothesis that the thermal drift originates from the thermal expansion of LVDT coils and the magnetic core, the new test rig intentionally locked down the relative position between these components. Preliminary finite element modeling in COMSOL Multiphysics confirmed the feasibility of the test rig. However, high-temperature characterization data collected at INL showed a significantly different result from the model prediction. The thermal drift resulting from the new LVDT test rig is nonlinear and at least two-orders higher in magnitude compared to previous TREAT reactor tests. Potential causes are: (1) The testing body wall is too thin and only allows for two threads to be engaged. Potential set screw slippage may have occurred at high temperature. This is supported by the changing starting point for each run. (2) The thermocouple did not fit inside of the test rig, causing an inaccuracy in temperature measurement. (3) Reference material rods may not achieve the proper tolerance, especially the assembly tolerance. Besides these potential mistakes, two additional challenges also hindered the data collection. First, it is extremely time consuming to reach the thermal equilibrium of the furnace. Second, assembly of the test rig was very difficult due to the wiring of the LVDT.

To tackle the experimental difficulties and fix the potential mistakes in previous tests, we plan to apply the following changes in FY-23: (1) The testing body thickness will be increased to allow at least three threads to be engaged with the set screw. (2) The holes on the end caps will be expanded to allow for thermocouple insertion. (3) The reference material rods and the magnetic core will be assembled through threads instead of laser welding to enhance axial alignment. In addition, we will remove the reference material rod on the left and collect thermal drift data with only one reference material rod. This approach should reduce the bending of the magnetic core.